Adaptation of pancreatic cancer cells to nutrient deprivation is reversible and requires glutamine synthetase stabilization by mTORC1

Pei-Yun Tsai[a,b,1], Min-Sik Lee[a,b,c,1], Unmesh Jadhav[d,e,f,g], Insia Naqvi[a], Shariq Madha[d,e], Ashley Adler[a,c], Meeta Mistry[h], Sergey Naumenko[h], Caroline A. Lewis[i], Daniel S. Hitchcock[j], Frederick R. Roberts[k], Peter DelNero[a,l], Thomas Hank[m], Kim C. Honselmann[m], Vicente Morales Oyarvide[d], Mari Mino-Kenudson[n], Clary B. Clish[j], Ramesh A. Shivdasani[d,e,f,g,o], and Nada Y. Kalaany[a,b,c,2]

[a]Division of Endocrinology, Boston Children's Hospital, Boston, MA 02115; [b]Department of Pediatrics, Harvard Medical School, Boston, MA 02115; [c]Broad Institute of MIT and Harvard, Cambridge, MA 02142; [d]Department of Medical Oncology, Dana-Farber Cancer Institute, Boston, MA 02215; [e]Center for Functional Cancer Epigenetics, Dana-Farber Cancer Institute, Boston, MA 02215; [f]Department of Medicine, Brigham and Women's Hospital, Boston, MA 02115; [g]Department of Medicine, Harvard Medical School, Boston, MA 02115; [h]Bioinformatics Core, Harvard T. H. Chan School of Public Health, Boston, MA 02115; [i]Metabolite Profiling Core Facility, Whitehead Institute for Biomedical Research, Cambridge, MA 02142; [j]Metabolomics Platform, Broad Institute of MIT and Harvard, Cambridge, MA 02142; [k]FUJIFILM VisualSonics Inc., Toronto, ON M4N 3N1, Canada; [l]Cancer Prevention Fellowship Program, Division of Cancer Prevention, National Cancer Institute, Bethesda, MD 20892; [m]Department of Surgery, Massachusetts General Hospital and Harvard Medical School, Boston, MA 02114; [n]Department of Pathology, Massachusetts General Hospital and Harvard Medical School, Boston, MA 02114; and [o]Harvard Stem Cell Institute, Cambridge, MA 02138

Edited by Matthew G. Vander Heiden, Koch Institute at MIT, and accepted by Editorial Board Member Anton Berns January 25, 2021 (received for review February 17, 2020)

Pancreatic ductal adenocarcinoma (PDA) is a lethal, therapy-resistant cancer that thrives in a highly desmoplastic, nutrient-deprived microenvironment. Several studies investigated the effects of depriving PDA of either glucose or glutamine alone. However, the consequences on PDA growth and metabolism of limiting both preferred nutrients have remained largely unknown. Here, we report the selection for clonal human PDA cells that survive and adapt to limiting levels of both glucose and glutamine. We find that adapted clones exhibit increased growth in vitro and enhanced tumor-forming capacity in vivo. Mechanistically, adapted clones share common transcriptional and metabolic programs, including amino acid use for de novo glutamine and nucleotide synthesis. They also display enhanced mTORC1 activity that prevents the proteasomal degradation of glutamine synthetase (GS), the rate-limiting enzyme for glutamine synthesis. This phenotype is notably reversible, with PDA cells acquiring alterations in open chromatin upon adaptation. Silencing of GS suppresses the enhanced growth of adapted cells and mitigates tumor growth. These findings identify nongenetic adaptations to nutrient deprivation in PDA and highlight GS as a dependency that could be targeted therapeutically in pancreatic cancer patients.

pancreatic cancer | nutrient deprivation | epigenetics | mTORC1 | glutamine synthetase

With a steady rise in incidence and a poor 5-y survival rate of ~9%, pancreatic ductal adenocarcinoma (PDA) is now the third leading cause of cancer death in the United States (1, 2). Oncogenic *KRAS* mutations are highly prevalent in PDA (>90%), driving many of its distinctive metabolic features (3, 4). These include the macropinocytic uptake of extracellular macromolecules, the recycling of intracellular components (5–8), and the redirection of glycolytic and glutaminolytic intermediates into anabolic and redox-controlling pathways required for PDA growth (9, 10). However, whether these alterations are sufficient to account for the ability of PDA to thrive in a seemingly hostile in vivo microenvironment, where abnormal vasculature and exuberant stroma restrict nutrient access, remains unknown.

Because nutrient availability largely dictates metabolic behavior (11), the relevance of studying tumor metabolism within the native environment has been recently underscored (12–16). Although culture media composition can be modulated to mimic circulating metabolite levels (17, 18), this modulation may not accurately reflect the tumor metabolic microenvironment. In particular, levels of glucose and glutamine, two of the most abundant and tumor-preferred nutrients in the circulation, can be limiting in PDA tumors, compared with benign adjacent tissue (7), and significantly lower within tumor cores, compared with the periphery (19, 20). Paradoxically, both glucose and glutamine are routinely supplemented in culture media at levels that are significantly higher than the circulation: 11 mM glucose and 2 mM glutamine in RPMI compared with ~5.5 mM glucose and 0.6 mM glutamine in serum (21). Although prior studies focused on depriving tumor cells of either glucose or glutamine alone (10, 22–25),

Significance

Pancreatic ductal adenocarcinoma (PDA) is a highly lethal malignancy with no effective therapies. PDA aggressiveness partly stems from its ability to grow within a uniquely dense stroma restricting nutrient access. This study demonstrates that PDA clones that survive chronic nutrient deprivation acquire reversible nongenetic adaptations allowing them to switch between metabolic states optimal for growth under nutrient-replete or nutrient-deprived conditions. One contributing factor to this adaptation is mTORC1 activation, which stabilizes glutamine synthetase (GS) necessary for glutamine generation in nutrient-deprived cancer cells. Our findings imply that although total GS levels may not be a prognostic marker for aggressive disease, GS inhibition is of high therapeutic value, as it targets specific cell clusters adapted to nutrient starvation, thus mitigating tumor growth.

Author contributions: R.A.S. and N.Y.K. designed research; P.-Y.T., M.-S.L., U.J., I.N., and A.A. performed research; U.J., M.M., S.N., C.A.L., D.S.H., F.R.R., P.D., T.H., K.C.H., M.M.-K., C.B.C., and R.A.S. contributed new reagents/analytic tools; P.-Y.T., M.-S.L., U.J., S.M., M.M., S.N., C.A.L., D.S.H., P.D., V.M.O., M.M.-K., and R.A.S. analyzed data; and N.Y.K. wrote the paper.

The authors declare no competing interest.

This article is a PNAS Direct Submission. M.G.V.H. is a guest editor invited by the Editorial Board.

See online for related content such as Commentaries.

[1]P.-Y.T. and M.-S.L. contributed equally to this work.

[2]To whom correspondence may be addressed. Email: nada.kalaany@childrens.harvard.edu.

This article contains supporting information online at https://www.pnas.org/lookup/suppl/doi:10.1073/pnas.2003014118/-/DCSupplemental.

Published March 2, 2021.

how PDA cells survive and proliferate under limiting levels of both major nutrients is not well understood.

To investigate this, we selected for clonal PDA cells that survive and adapt to limiting levels of both glucose and glutamine. We find that the adapted clones have enhanced proliferation in vitro and tumor-forming capacity in vivo. They also share common signaling, transcriptional, and metabolic alterations that are acquired upon adaptation. These include a posttranslational role for mTORC1 signaling in the stabilization of glutamine synthetase (GS), and the use of amino acids for the synthesis of glutamine and nucleotides. Of note, this phenotype is reversible, implicating epigenetic alterations in the adaptation process, and highlighting GS as a candidate for therapeutic targeting in pancreatic cancer.

Results

PDA Cells Adapted to Low Glucose/Low Glutamine Have Enhanced Growth In Vitro and In Vivo. To test whether pancreatic cancer cells can survive and adapt to harsh nutrient-deprived conditions, we cultured seven human PDA cell lines (AsPC-1, BxPC-3, HPAC, MIA PaCa-2, PANC-1, SUIT-2, and PA-TU-8988T, herein termed 8988T) in customized low glucose (0.5 mM) and low glutamine (0.1 mM), medium (L-L). These modifications represent an ∼20-fold reduction from standard RPMI medium, herein referred to as high glucose-high glutamine (H-H) and a 5- to 10-fold decrease from human serum levels (21) (Fig. 1*A*); both L-L and H-H media were supplemented with 10% dialyzed fetal bovine serum (FBS). Consistent with the requirement of glucose and glutamine for PDA growth (9, 10), most PDA cells died within 2 wk of culture in L-L medium, despite media replenishment every 2 to 3 d (Fig. 1*B* and *SI Appendix*, Fig. S1*A*). However, rare surviving cells were able to slowly proliferate past the second week, particularly in SUIT-2 and 8988T, followed by MIA-PaCa-2 (Fig. 1*B* and *SI Appendix*, Fig. S1*B*). Distinct genetic lesions frequently found in PDA did not explain the differential adaptive capacity of these cell lines to nutrient deprivation (*SI Appendix*, Fig. S1*C*). The surviving cells in SUIT-2 and 8988T gradually gave rise to adapted clones, three of which (A-C4, C-5, and C-6) were selected for further analysis (Fig. 1*A*). Adapted clones were then studied in comparison with nonadapted clones (NA-C1, C-2, and C-3), which were isolated from the corresponding parental PDA lines grown under H-H conditions (Fig. 1*A*). All clones were subsequently passaged every 3 to 4 d for use in experiments.

To assess their in vitro growth potential, adapted and nonadapted cells were first subjected to a 7-d proliferation assay performed without media replenishment, which is expected to lead to a halt in proliferation or drop in cell number by day 7, given nutrient depletion. Whereas no significant differences were detected in H-H medium conditions (*SI Appendix*, Fig. S2 *A* and *B*), adapted cells from both lines showed enhanced proliferative capacity (Fig. 1*C*) and decreased cell death (Fig. 1*D* and *SI Appendix*, Fig. S2*C*), compared with nonadapted clones, in L-L medium. In a colony formation assay, adapted clones tended to generate a larger number of colonies in L-L but not in H-H medium (Fig. 1*E* and *SI Appendix*, Fig. S2*D*). When plated under three-dimensional (3D) culture conditions, adapted 8988T cells formed a significantly higher number of spheres (*SI Appendix*, Fig. S2*E*) with a larger area (Fig. 1*F*) than nonadapted clones in L-L, but not H-H medium (*SI Appendix*, Fig. S2 *F* and *G*). SUIT-2 clones formed a similar number of spheres, independent of the medium or adaptation (*SI Appendix*, Fig. S2 *E* and *F*). However, SUIT-2 spheres tended to be larger in adapted compared with nonadapted clones, when cultured under L-L, but not H-H conditions (Fig. 1*F* and *SI Appendix*, Fig. S2*G*).

Because autophagy and macropinocytosis are well-recognized dependencies in PDA (3, 5, 6, 8), we assessed their potential contribution to the enhanced proliferation of the adapted clones under nutrient-limiting conditions. No differential increase in autophagic flux was observed in adapted cells compared with nonadapted controls in L-L medium (*SI Appendix*, Fig. S3*A*). Moreover, uptake of tetramethylrhodamine (TMR)-labeled dextran, an indicator of macropinocytosis, was not further increased in the adapted compared with nonadapted cells, under L-L conditions (*SI Appendix*, Fig. S3*B*). These data indicate that surviving PDA cells that adapt to chronic glucose and glutamine deprivation acquire a proliferative potential that depends on processes other than autophagy or macropinocytosis.

To test whether the adaptation-mediated in vitro phenotype could be translated in vivo, adapted and nonadapted SUIT-2 PDA clonal cells were orthotopically injected into the pancreas of B6.Rag1$^{-/-}$ mice (Fig. 1 *G* and *H* and *SI Appendix*, Fig. S2*H*). Within the span of 6 wk, only 8 out of 13 nonadapted cell injections derived from two different clones formed detectable, yet smaller tumors (∼119 mm^3 in volume; 197 mg in weight) with delayed latency (Fig. 1 *G* and *H*). In contrast, 14 of 14 adapted clonal cell injections produced tumors that were detected as early as week 3 by ultrasound (Fig. 1*G*). At week 6, these tumors were approximately fourfold larger in volume (∼463 mm^3) and over twofold heavier (∼436 mg) than tumors from nonadapted clones (Fig. 1 *G* and *H* and *SI Appendix*, Fig. S1*G*). Moreover, two mice bearing the largest tumors from adapted cells (Fig. 1*G*, clone 5, red arrow) succumbed to tumor burden at week 5 and were therefore not included in the analyses at week 6 (Fig. 1 *G* and *H*). These results demonstrate that metabolic adaptation to a nutrient-deprived environment can endow cancer cells with higher growth fitness, allowing tumors to survive and thrive during periods of nutrient starvation both in vitro and in vivo.

Adapted PDA Clones Display Altered Amino Acid and Nucleotide Metabolism Coupled with Enhanced mTORC1 Signaling. To identify transcriptional alterations that convey enhanced proliferative potential to PDA upon adaptation to nutrient deprivation, we used RNA sequencing (RNA-Seq) to profile transcripts in SUIT-2 clones under L-L conditions. Gene set enrichment analysis (GSEA) revealed significant enrichment in the adapted clones for pathways involved in purine and pyrimidine metabolism (*SI Appendix*, Fig. S4 *A* and *B*), amino acid metabolism (*SI Appendix*, Fig. S4 *C*–*F*), as well as mammalian target of rapamycin complex 1 (mTORC1) signaling (*SI Appendix*, Fig. S4*G*). Metabolic profiling of SUIT-2 clones treated for 24 h with H-H or L-L medium yielded an adaptation signature that largely overlaps with the altered transcriptomes (*SI Appendix*, Fig. S5 *A* and *B*). Compared with H-H, all clones under L-L conditions displayed markedly higher levels of intracellular amino acids (*SI Appendix*, Fig. S5*A*), except for alanine, glutamine, glutamate, and aspartate, consistent with glutamine deprivation and indicative of enhanced autophagy. This increase in amino acids was significantly suppressed in the adapted clones compared with nonadapted controls, suggesting enhanced utilization of intracellular amino acids (*SI Appendix*, Fig. S5*A*). Furthermore, nonadapted cells showed significant accumulation of mono- and dinucleotides and their biosynthetic precursors, reflecting decreased DNA synthesis. In contrast, the adapted clones displayed a nucleotide biosynthesis profile that closely mirrors that of PDA clones under H-H conditions, consistent with enhanced proliferation. This profile included lower levels of mono- and dinucleotide phosphates, used to generate trinucleotide phosphates, which differentially accumulate in the adapted clones (Fig. 2*A*, relative levels between two groups in L-L and *SI Appendix*, Fig. S5*A*, relative levels among four groups in L-L and H-H). Indeed, although de novo pyrimidine synthesis was higher under H-H compared with L-L conditions, a differential increase upon adaptation was observed only under L-L conditions (Fig. 2*B*). This was evident in doubling of ^{14}C incorporation into DNA, 40 h after labeling of cells with ^{14}C-aspartate (Fig. 2*B*).

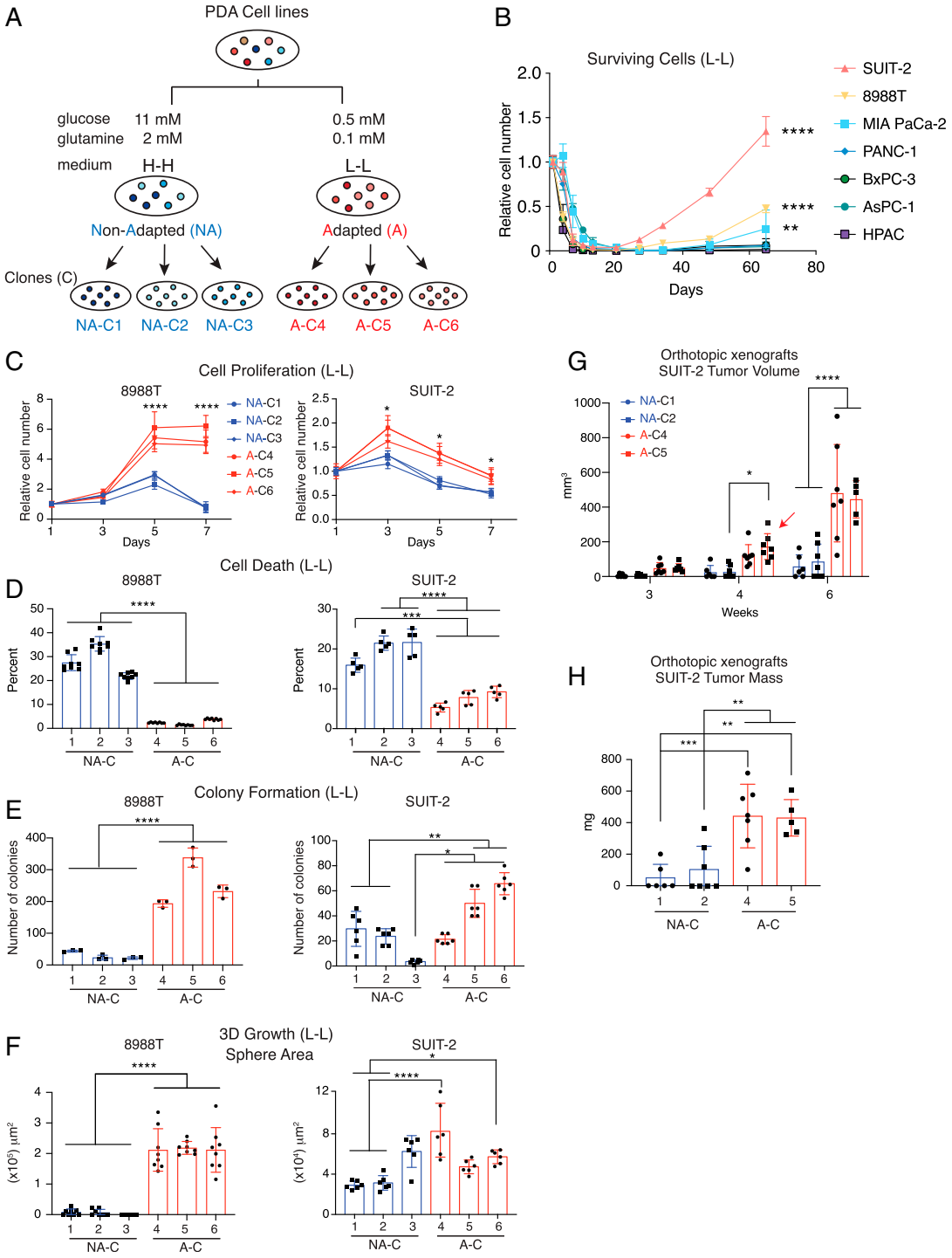

Fig. 1. PDA cells adapted to nutrient deprivation exhibit enhanced growth in vitro and in vivo. (*A*) Schematic depicting the adaptation process to glucose and glutamine deprivation, followed by selection of adapted "A" clones (C4 to C6) derived from SUIT-2 or 8988T human PDA cells that survived and grew in low glucose-low glutamine (L-L) medium, and control nonadapted "NA" clones (C1 to C3) derived from parental cells plated at low dilution in high glucose-high glutamine (H-H) medium. (*B*) Relative number of surviving cells from all seven PDA cell lines that were subjected to L-L medium for a period of 65 d ($n = 3$). (*C*) Proliferation curves of clonal cells described in *A* that were grown in L-L medium for 7 d ($n = 5$ for SUIT-2 and $n = 8$ for 8988T). (*D*) Percent cell death in clones described in *A* ($n = 5$ for SUIT-2 and $n = 8$ for 8988T) that was quantified on day 4 (SUIT-2) or day 5 (8988T) of growth in L-L medium. (*E*) Colony formation assay showing number of colonies formed by SUIT-2 or 8988T clones described in *A* that were grown in L-L medium for 7 d ($n = 6$ for SUIT-2 and $n = 3$ for 8988T). (*F*) Three-dimensional growth assay showing area of spheres formed by SUIT-2 or 8988T cells described in *A* that were grown for 7 d or 10 d, respectively, in L-L medium supplemented with 4% Matrigel ($n = 6$ for SUIT-2 and $n = 8$ for 8988T). (*G*) Volumes of orthotopic xenograft PDA tumors quantified by ultrasound that were derived from SUIT-2 clones described in *A* and injected (750×10^3 cells) into the pancreas of 4- to 6-wk-old Rag1$^{-/-}$ mice. Tumors were grown for 43 d ($n = 7$ except for NA-C1, $n = 6$); red arrow points at the two largest A-C5 tumors at week 4 from mice that died before the week 6 endpoint. (*H*) Weights of orthotopic xenograft SUIT-2 tumors described in *G* that were analyzed at the endpoint, 6 wk posttumor cell injection. Data represent the mean ± SEM in *B* and *C*, or mean ± SD in *D*–*H*. *$P < 0.05$; **$P < 0.01$; ***$P < 0.001$; ****$P < 0.0001$, two-way ANOVA for *B*, *C*, and G and one-way ANOVA for (*D*, *F*, and *H*) followed by a Tukey test.

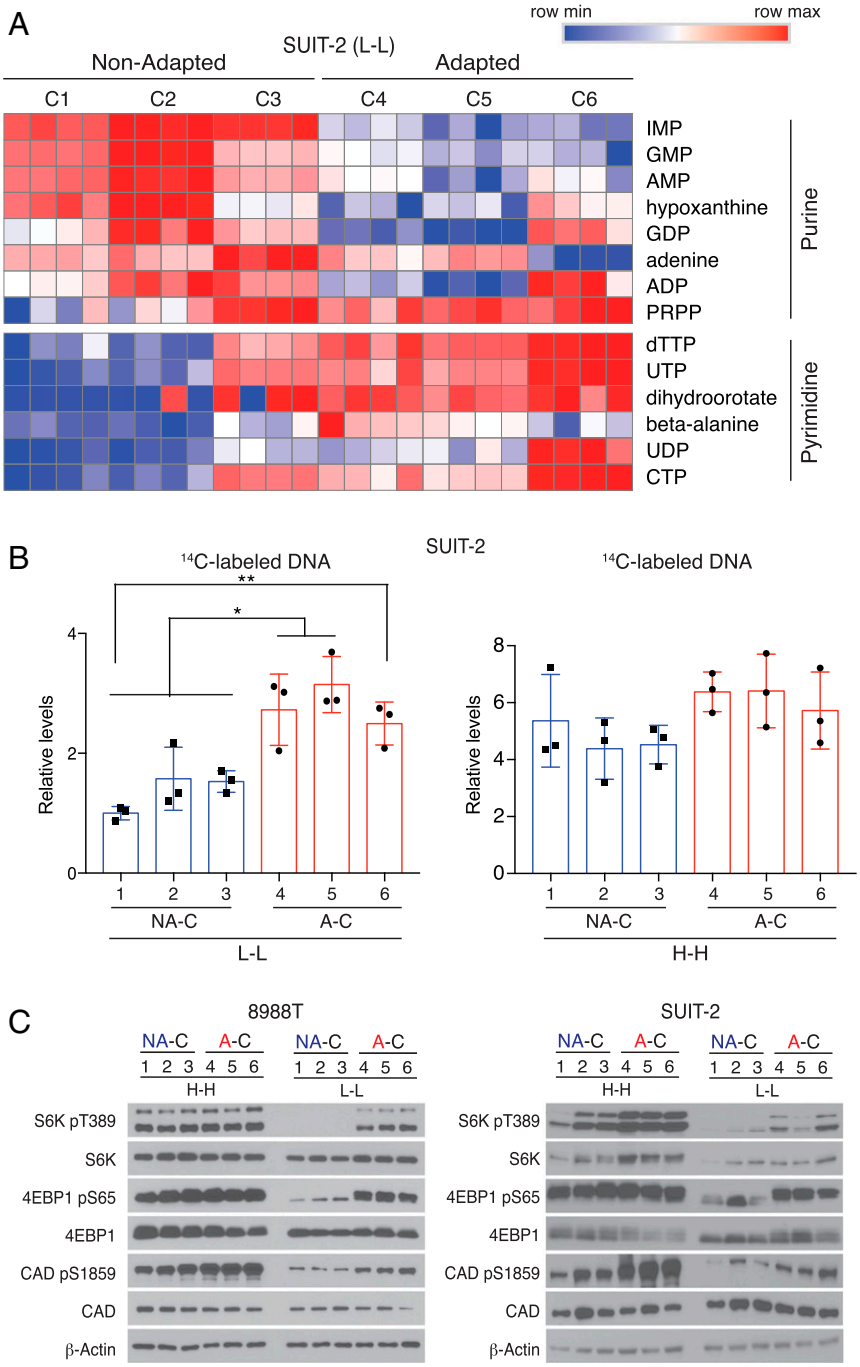

Fig. 2. Adapted PDA clones display enhanced de novo DNA synthesis and mTORC1 signaling under nutrient-deprived conditions. (*A*) Heatmap listing in descending order of statistical significance ($P < 0.05$ by *t* test) metabolites in the purine and pyrimidine synthesis pathways for nonadapted (C1 to C3) or adapted (C4 to C5) SUIT-2 clones that were treated for 24 h with L-L medium ($n = 4$ replicates per clone). Red indicates higher level and blue lower level, relative to the median for each metabolite across all groups. (*B*) Relative incorporation of radiolabeled U-^{14}C-aspartate into DNA synthesis in nonadapted (NA-C) and adapted (*A*–*C*) SUIT-2 clones treated with either L-L or H-H medium for 40 h. Data are presented as relative fold change normalized to NA-C1 under L-L conditions and represent the mean ± SD ($n = 3$ replicates per clone). *$P < 0.05$; **$P < 0.01$, one-way ANOVA followed by a Tukey test. (*C*) Immunoblots of pT389-S6K, pS65-4EBP1, pS1859-CAD, and total S6K, 4EBP1, CAD in SUIT-2 or 8988T clones treated with H-H or L-L medium for 24 h. β-Actin was used as loading control.

Signaling downstream of mTORC1 can induce de novo pyrimidine synthesis through activation of the rate-limiting enzyme "CAD" (carbamoyl-phosphate synthetase 2, aspartate transcarbamoylase, dihydroorotase) (26). Since GSEA also indicated a potential increase in mTORC1 activity in adapted clones under L-L conditions (*SI Appendix*, Fig. S4*G*), we investigated a role for mTORC1 in the adaptation of the PDA clones to nutrient deprivation. Compared with nonadapted clones, adapted SUIT-2

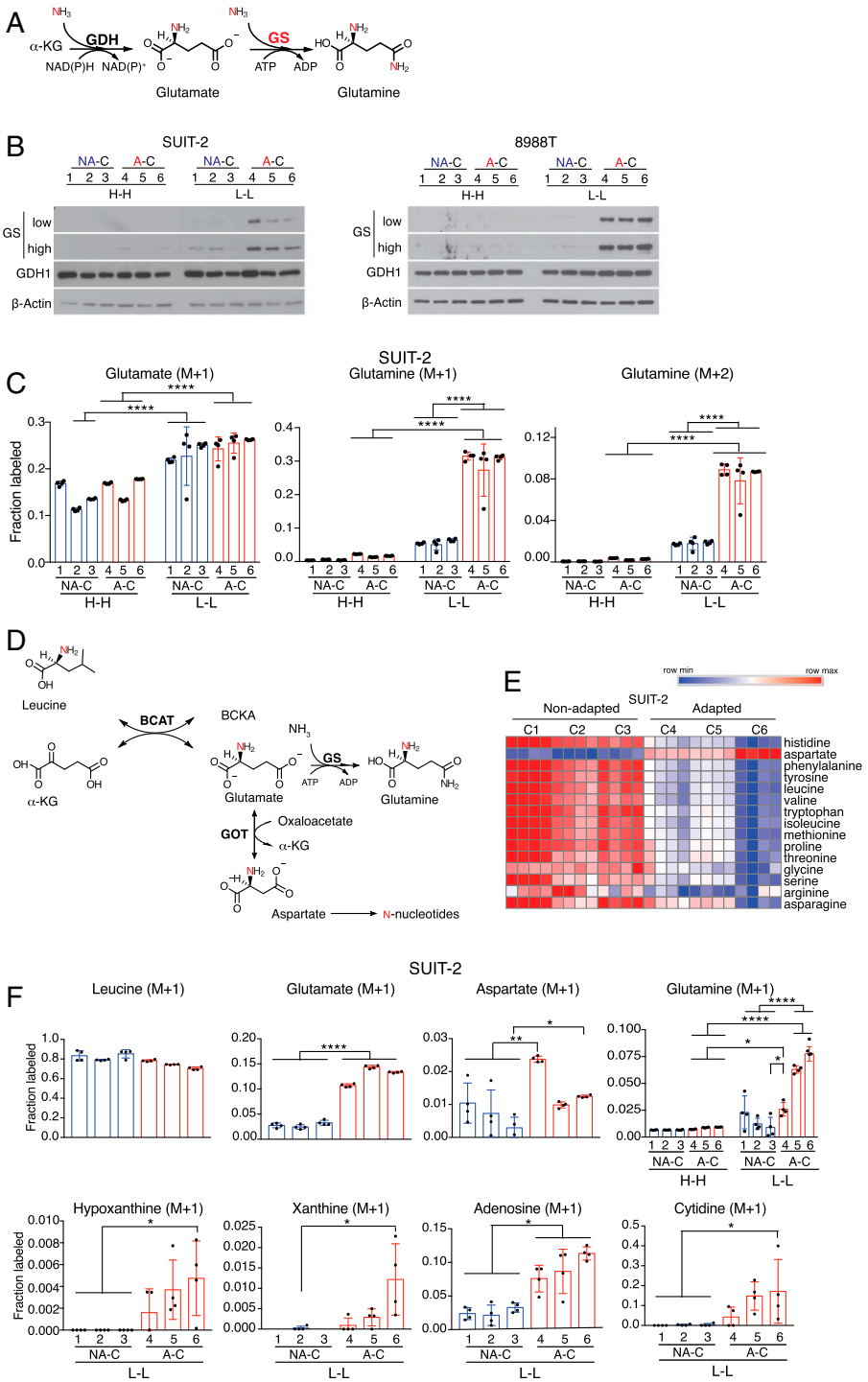

Fig. 3. Adapted PDA cells induce GS and have enhanced incorporation of nitrogen from amino acids into glutamine and nucleotide synthesis. (*A*) Schematic illustrating glutamate synthesis from α-ketoglutarate (α-KG) and ammonia by glutamate dehydrogenase (GDH) and glutamine synthesis from glutamate and ammonia by glutamine synthetase (GS). In red, are ammonia nitrogens incorporating into glutamate and then glutamine. (*B*) Immunoblots of GS (low and high exposures) and GDH in SUIT-2 or 8988T clones treated with H-H or L-L medium for 24 h. β-Actin was used as loading control. (*C*) Fractional labeling of ^{15}N-glutamate and glutamine in SUIT-2 cells treated for 24 h with H-H or L-L medium supplemented with 0.8 mM ^{15}N-ammonium chloride. Data are corrected for natural abundance and represent the average of four replicates per clone per condition ± SD. (*D*) Schematic illustrating the incorporation of leucine nitrogen (red) into glutamate and then aspartate via transamination reactions catalyzed by branched chain amino acid transaminase BCAT and aspartate transaminase GOT. Glutamate is used to synthesize glutamine via GS and aspartate nitrogen incorporates into newly synthesized nucleotides. (*E*) Heatmap listing in descending order of statistical significance ($P < 0.05$ by *t* test) amino acids in nonadapted or adapted SUIT-2 clones that were treated for 24 h with L-L medium ($n = 4$ per clone per condition). Red indicates higher level and blue lower level, relative to the median for each metabolite across all groups. (*F*) Fractional labeling of metabolites in glutamine and nucleotide synthesis pathways in cells described in *B* grown in media supplemented with 0.4 mM ^{15}N-leucine for 24 h. Data represent the average of four replicates per clone per condition ± SD *$P < 0.05$; **$P < 0.01$; ****$P < 0.0001$, two-way ANOVA for *C*, one-way ANOVA for *F* except for "glutamine" (two-way ANOVA), followed by a Tukey test.

and 8988T cells showed increased phosphorylation levels of CAD on serine 1859, a site of ribosomal S6-kinase (S6K1) activity (Fig. 2*C*). This increase was particularly striking under L-L conditions. Importantly, it was mirrored by enhanced mTORC1 activity, as evidenced by sustained phosphorylation of its downstream effectors S6K1 and 4E-binding protein (4E-BP1), despite nutrient deprivation (Fig. 2*C*). On the other hand, no significant changes were detected in the phosphorylation levels of ERK1/2 downstream of activated KRAS. Moreover, levels of AKT phosphorylation (T308) were decreased in adapted clones (*SI Appendix*, Fig. S6), consistent with mTORC1-AKT negative feedback loops (27–29).

Adapted PDA Clones Have Enhanced Glutamine Synthesis. Glutamine is a pleiotropic amino acid required for protein synthesis and numerous anabolic reactions in proliferating cells (22). We therefore asked whether the adapted clones have induced de novo glutamine synthesis under L-L conditions. mRNA levels of glutamine synthetase (GS, also termed GLUL), which catalyzes the condensation of glutamate and ammonium to generate glutamine (Fig. 3*A*), were only moderately increased in adapted clones (*SI Appendix*, Fig. S7*A*). However, GS protein levels were markedly induced in adapted clones from both PDA cell lines, compared with nonadapted controls (Fig. 3*B*). This occurred only under L-L conditions, as no clones harbored detectable levels of GS in H-H medium, independent of adaptation (Fig. 3*B*). Although these findings are consistent with a glutamine-dependent posttranslational regulation of GS (30, 31), it is noteworthy that nonadapted clones only displayed a mild-to-no increase in GS levels 24 h following exposure to L-L medium (Fig. 3*B*), implying differential metabolic rewiring in the PDA clones upon adaptation to prolonged glutamine deprivation. Importantly, GS protein levels were mirrored by its enzymatic activity levels, as demonstrated by metabolic tracing of ^{15}N-ammonium chloride (NH_4Cl) in SUIT-2 cells (Fig. 3*C*). Because glutamate dehydrogenase (GDH, also termed GLUD) catalyzes the reductive amination of alpha-ketoglutarate (α-KG) to generate glutamate (Fig. 3*A*), a moderate increase was observed in the ^{15}N-glutamate fraction between H-H and L-L conditions in SUIT-2 cells (~18% vs. 25%), independent of adaptation (Fig. 3*C*). This suggested the use by the adapted cells of newly generated glutamate to synthesize glutamine. Indeed, adapted clones cultured in L-L medium had a marked increase in ^{15}N-glutamine (M+1) fraction, generated from either condensation of ^{15}N-ammonium and unlabeled glutamate, or unlabeled ammonium and GDH-derived ^{15}N-glutamate, compared with nonadapted controls (30% vs. 8%, respectively). This increase was also observed in the (M+2) labeled fraction, which is generated when both substrates are labeled (8% in adapted vs. 2% in nonadapted cells). On the other hand, ^{15}N-glutamine levels were either undetectable or minimally detected in the PDA clones under H-H conditions, independent of adaptation (Fig. 3*C*). These data indicate that only PDA clones that survive and adapt to long-term glutamine deprivation are able to induce GS protein levels under L-L conditions, so as to increase GS-mediated glutamine synthesis.

Adapted PDA Cells Use Amino Acids as a Nitrogen Source for Glutamine and Nucleotide Synthesis. In addition to reductive amination of α-KG through GDH (Fig. 3*A*), the transamination reaction catalyzed by branched chain amino acid (BCAA) transaminase (BCAT1/2) could contribute to the generation of mitochondrial glutamate that is then used for glutamine synthesis. Moreover, aspartate transaminase (GOT1/2, also termed AST1/2) could transfer the nitrogen from glutamate to aspartate, a key substrate in nucleotide biosynthesis (Fig. 3*D*). Global metabolite profiling of the PDA clones revealed a significant decrease in amino acid levels, including the BCAAs leucine, valine, and isoleucine in all adapted clones, suggesting enhanced amino acid utilization by the more proliferative cells (see Fig. 3*E* for relative levels between 2 groups in L-L and *SI Appendix*, Fig. S5*A* for relative levels among all 4 groups in H-H and L-L). Indeed, adapted clones showed increased protein levels of BCAT2 and GOT2 in SUIT-2 cells, whereas BCAT1 and GOT1 were increased in 8988T cells (*SI Appendix*, Fig. S7*B*). ^{15}N-leucine tracing demonstrated that the labeled nitrogen incorporates at significantly higher levels into glutamate, aspartate, and intermediates in nucleotide synthesis in adapted compared with nonadapted clones under L-L conditions (Fig. 3*F*). Moreover, the ^{15}N-labeled fraction of glutamine was minimal (1%) under nutrient-replete H-H conditions, whereas a marked fivefold increase in ^{15}N-glutamine was detected under L-L conditions, specifically in the adapted clones (Fig. 3*F*). These data imply that BCAAs are a significant source for de novo synthesis of glutamine and nucleotides in PDA cells adapted to L-L conditions.

Deprivation of Glutamine rather than Glucose Is a Larger Contributor to the Enhanced Proliferative Fitness of Adapted PDA Cells. To distinguish the contributions of glucose versus glutamine to the adaptability phenotype, we selected for SUIT-2 and 8988T parental cells that survive and adapt to deprivation of either glucose-only (low glucose-high glutamine; L-H medium), glutamine-only (high glucose-low glutamine; H-L medium), or both glucose and glutamine (L-L). We then compared their proliferative capacity with that of control nonadapted parental cells that were maintained in nutrient replete (H-H) medium. Under H-H medium, enhanced proliferation of adapted cells was observed only on the last day of the assay (day 7), when nutrients become more depleted in the nonreplenished medium (*SI Appendix*, Fig. S8 *A*, *Top*). When grown in L-L medium, however, the markedly enhanced proliferative capacity of cells adapted to L-L conditions could be mostly attributed to adaptation to glutamine deprivation, rather than deprivation of glucose. This is evident in the growth curves of H-L adapted cells that more closely mimic those of L-L adapted cells; in contrast, L-H adapted cells only displayed minimal to moderately enhanced proliferative fitness (*SI Appendix*, Fig. S8 *A*, *Bottom*). Consistently, GS protein levels were most induced in H-L compared with L-H adapted clones in both cell lines (*SI Appendix*, Fig. S8*B*).

We next assessed the effects of short-term deprivation of either glucose or glutamine, on altered metabolism, mTORC1 activity, and GS levels in the L-L adapted SUIT-2 clones (Fig. 1*A*). Except for metabolites in glycolysis (marked with a star), deprivation of glutamine alone (H-L), rather than glucose (L-H), more closely mimicked the metabolic alterations observed upon deprivation of both nutrients (L-L). These include changes in levels of amino acids, tricarboxylic acid (TCA) cycle metabolites, and nucleotides (*SI Appendix*, Fig. S9). Moreover, whereas loss of either glucose or glutamine or both for 24 h, strongly suppressed mTORC1 signaling in nonadapted clones, adapted cells maintained significant mTORC1 activity even in the absence of glucose, but particularly under low glutamine conditions (H-L or L-L). Similarly, GS induction was highly dependent on both adaptation status and glutamine levels, with adapted clones displaying highest GS protein levels under H-L or L-L conditions (*SI Appendix*, Fig. S8*C*, with levels normalized and quantified in *D*). This led us to investigate a possible genetic basis for induced mTORC1 activity in the adapted clones and a potential role for mTORC1 in inducing GS levels under low glutamine conditions.

mTORC1 Activation and Enhanced Proliferative Potential Are Reversible in Adapted PDA Clones. Because the adapted clones sustain active mTORC1 signaling independent of nutrient deprivation, we asked whether the adaptation process had selected for cells with inherent mutations that constitutively activate mTORC1. We first cultured the SUIT-2 adapted clones in nutrient-replete H-H medium for four or

more consecutive passages (a process we termed "adaptation reversal") followed by treatment for 24 h with L-L medium (Fig. 4*A*). Reverse-adapted (RA) clones displayed gradual suppression of mTORC1 activity (Fig. 4*B*), indicating that the enhanced anabolic signaling acquired upon adaptation is an unlikely result of genetic mutations selected for in the adapted clones. This was later confirmed with whole exome sequencing (WES) analysis that found no high or moderate impact mutations (*Materials and Methods*) in any of the genes in the mTORC1 signaling pathway (Dataset S1) that was identified as enriched at the transcriptional level, by GSEA (*SI Appendix*, Fig. S4*G*). Indeed, of all 23 genes (*SI Appendix*, Fig. S4*G*), only 10 genetic variants exist that were found however in all clones, independent of adaptation (C1 to C9, Dataset S1). Consistently, adapted and RA clones clustered according to clone number (*SI Appendix*, Fig. S10*A*) rather than according to adaptation, with no high impact mutations found in whole exome variants, implying that genetic differences acquired upon reverse adaptation were minimal (*SI Appendix*, Fig. S10*A* and Dataset S2).

Importantly, in vitro survival and growth of adapted clones were partially reversed, with all RA clones exhibiting decreased proliferation compared with adapted clones, and one RA clone displaying a trend in enhanced cell death (Fig. 4 *C* and *D*). Furthermore, among a pool of 1,842 genes whose expression was significantly altered (threefold or more change, $q < 0.05$) upon adaptation, about half of the changes were partially reversed in RA clones (clusters I, II, and V, Fig. 4*E*), consistent with decreased mTORC1 signaling and proliferative capacity (Fig. 4 *B* and *C*). These results imply that adaptation to nutrient deprivation depends on a fraction of the transcriptional changes that accompany it.

Inactive gene regulatory elements tend to be inaccessible (closed chromatin), in contrast to active cis-elements, which reside in open chromatin (32). To investigate a potential epigenetic basis for the adaptation of PDA cells to nutrient deprivation, we asked whether the transcriptional changes were associated with chromatin dynamics. Assays for transposase-accessible chromatin with high throughput sequencing (ATAC-Seq) identified a significantly altered landscape of open chromatin in adapted clones compared with nonadapted clones, including gains and losses of chromatin accessibility near thousands of enhancers (Fig. 4*F*). Adaptation-related increases in chromatin access correlated with increased mRNA levels and conversely, reduced chromatin access correlated with lower mRNA levels (Fig. 4*G* and *SI Appendix*, Fig. S10*B*). Notably, alterations in open chromatin were largely preserved in reverse-adapted cells (Fig. 4*F* and *SI Appendix*, Fig. S10 *C*, *Left*) with infrequent reversion (Fig. 4*F* and *SI Appendix*, Fig. S10 *C*, *Right*). Thus, most changes in chromatin accessibility are stable, and again, adaptation depends only on a fraction of them. Further reversal of open chromatin changes, with corresponding changes in gene expression and near complete reversal of proliferative fitness, may require prolonged deadaptation of PDA clones in nutrient-replete media.

mTORC1 Prevents Proteasomal Degradation of GS in Adapted PDA Clones. Because the induction of GS protein in adapted cells consistently mirrored mTORC1 signaling (Figs. 2*C* and 3*B* and *SI Appendix*, Fig. S8 *B* and *C*), including reversibility upon deadaptation (Fig. 4*B*), we asked whether mTORC1 regulates GS levels. Upon treatment with the mTOR kinase inhibitor Torin1, *GS* mRNA levels were increased in adapted clones under L-L conditions (*SI Appendix*, Fig. S11*A*). In contrast, consistent with posttranscriptional GS regulation, Torin1 markedly decreased GS protein levels (Fig. 5*A*). This decrease was not observed upon treatment with cycloheximide, but only when Torin1 was added to the cells, indicating that mTORC1 regulation of GS is posttranslational (Fig. 5*B* and *SI Appendix*, Fig. S11*B*). Indeed, whereas treatment with the proteasomal inhibitor MG-132 did not significantly affect GS levels in adapted clones over 2 to 8 h, it induced GS at the 8-h timepoint in nonadapted cells treated with L-L media (Fig. 5*C*), despite suppressed activity of the translational regulator mTORC1 under these conditions (Fig. 2*C*). Importantly, the Torin1-induced decrease in GS levels in adapted cells was rescued upon treatment with MG-132 (Fig. 5*D*). Furthermore, mTORC1 inhibition promoted GS polyubiquitination, as evidenced in immunoprecipitated GS from adapted cells cotreated with Torin1 and MG-132 (Fig. 5*E*). Altogether, these data demonstrate that GS is ubiquitinated and targeted for proteasomal degradation in nonadapted clones, even under L-L conditions, and that mTORC1 prevents this degradation, leading to GS stabilization in adapted clones.

PDA Cells Adapted to Nutrient-Deprived Conditions Are Sensitive to GS Inhibition. To assess the contribution of glutamine synthesis to the enhanced growth of the adapted cells, PDA clones were treated with the GS inhibitor L-methionine sulfoximine (MSO). Adapted cell proliferation was mitigated under L-L, but not H-H conditions, underscoring the relevance of glutamine synthesis in the nutrient-deprived state (*SI Appendix*, Fig. S12*A*). Genetic silencing of GS similarly suppressed adapted cell proliferation and colony formation (Fig. 6 *A–C* and *SI Appendix*, Fig. S12 *B–D*). To ask whether the contribution of GS to enhanced in vitro PDA growth extends in vivo, we induced knockdown of GS in orthotopic PDA transplants (Fig. 6 *D* and *E*). Five days following injection of adapted SUIT-2 cells expressing control or *GS* hairpins into the pancreas, gene silencing was induced by treating mice with doxycycline (Dox) in the drinking water. Two distinct *GS* hairpins attenuated PDA growth (Fig. 6*D* and *SI Appendix*, Fig. S12 *E* and *F*), resulting in 6.1- to 9.2-fold lower tumor weights upon Dox treatment (Fig. 6*D*). Although no significant changes in apoptosis were detected at the experimental endpoint, *Ki*-67 proliferative index tended to be moderately lower in tumors upon GS knockdown (*SI Appendix*, Fig. S12 *G* and *H*). Altogether, our results indicate that GS-mediated glutamine synthesis is required for PDA cells to survive and adapt to the characteristic nutrient-deprived PDA environment and highlight GS as a metabolic target in treating pancreatic cancer (Fig. 6*F*).

To extend our findings to human pathology, tissue microarrays (TMAs) of resected tumors from 127 pancreatic cancer patients were immunostained and scored for GS protein levels. As a reference for intensity, stained control cores of normal pancreas showed high GS levels in islets and modest levels in acinar cells. Within tumor cores, PDA cells displayed heterogeneous cytoplasmic staining that varied widely from strong to moderate to weak, with an overall score lower than that of acinar cells. As a result, no significant association was found between PDA GS levels and tumor size, lymph node involvement (pT or pN staging, the American Joint Commission on Cancer, AJCC eighth edition) (33) or patient survival (*SI Appendix*, Fig. S13 *A–C*). Although these results seem discordant with a recent report that GS expression is a feature of *KRAS*-driven PDA (34), the pathological heterogeneity and variability in GS protein levels is consistent with an inverse correlation with nutrient deprivation (Figs. 3 and 4 and *SI Appendix*, Fig. S8). Indeed, nutrient distribution is recognized to be heterogeneous in the tumor microenvironment, with glutamine levels being most depleted within tumor cores, compared with the periphery (19, 20). Therefore, future studies could confirm whether gradients of GS protein levels exist among distinct PDA cell clusters within the tumor mass, depending on their precise location and proximity to blood vessels. Nevertheless, based on our results and those of Bott et al. (34), targeting GS in the nutrient-deprived PDA tumors holds significant therapeutic value in pancreatic cancer.

Discussion

The in vitro dependence of proliferating cells on glutamine (22) was recently questioned in the in vivo setting, where tumors preferably utilize glucose and other metabolites, rather than

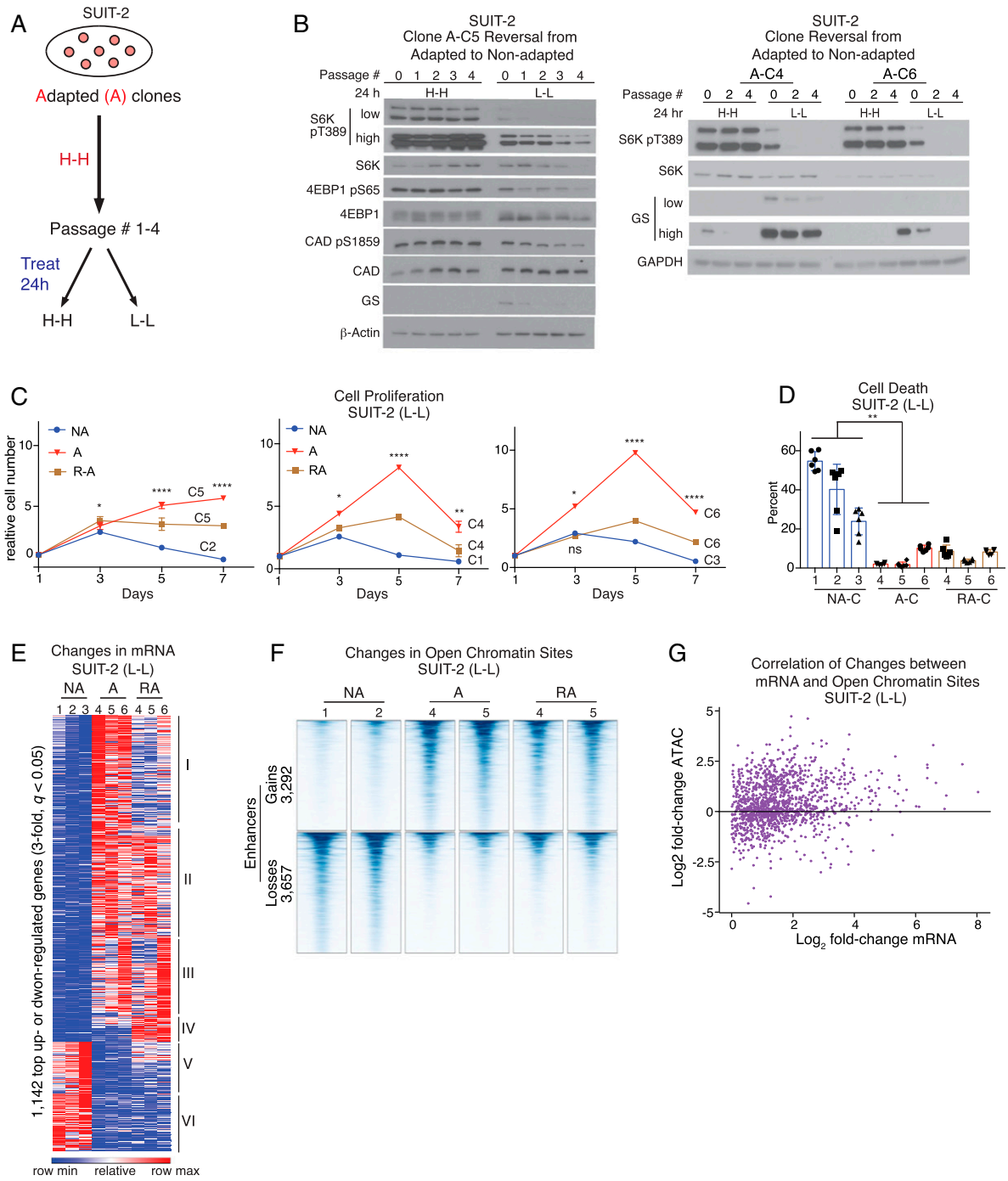

Fig. 4. PDA adaptation to nutrient deprivation is reversible and associated with changes in open chromatin. (*A*) Schematic depicting the adaptation reversal process where adapted PDA SUIT-2 clones are grown in nutrient replete (H-H) conditions for at least 4 passages, prior to treatment with H-H or L-L medium for 24 h. (*B*) Immunoblots of pT389-S6K (low and high exposures), pS65-4EBP1, pS1859-CAD, and total S6K, 4EBP1, CAD, and GS (low and high exposures) in SUIT-2 clones (C5, C4, and C6) that were reverse adapted for over 4 passages and then treated with H-H or L-L medium for 24 h. β-Actin or GAPDH was used as loading control. (*C*) Proliferation curves of SUIT-2 clones C5, C4, and C6 from *B* that are either adapted "A" or reverse adapted "RA" for 18 passages, as compared with nonadapted "NA" clones C2, C1, or C3. All clones were grown under L-L conditions for 7 d without media replenishment ($n = 6$). (*D*) Percent cell death in clones described in *C* that were grown under L-L medium for 5 d ($n = 6$). Data represent the mean ± SEM in *C*, and mean ± SD in *D*. $^*P < 0.05$; $^{**}P < 0.01$; $^{****}P < 0.0001$, two-way ANOVA for *C* and one-way ANOVA for *D*, followed by a Tukey test. In *C*, stars indicate statistical significance for A vs. NA; A vs. RA; RA vs. NA on the indicated days. (*E*) Relative mRNA levels of 1,842 genes that were either up-regulated or down-regulated (more than threefold, $q < 0.05$) in SUIT-2 adapted clones compared with nonadapted clones; mRNA levels of the corresponding genes in "RA" clones (reverse-adapted for 9 passages), are shown alongside. All clones were treated for 24 h with L-L medium. Differentially expressed genes were identified by unsupervised *k*-means clustering. Red, high expression; blue, reduced expression relative to mean expression levels for each gene across all groups ($n = 3$ clones per group). (*F*) ATAC-Seq data showing significant (more than twofold, $q < 0.05$) changes in chromatin access at enhancers (located >500 bp from transcription start sites) in each of two independent SUIT-2 clones that were either nonadapted (NA), adapted (A), or reverse-adapted (RA) for 5 passages. All clones were treated for 24 h with L-L medium. (*G*) Correlation of changes in gene expression and nearby (<25 kb) chromatin accessibility for the genes that were induced upon adaptation to nutrient deprivation in SUIT-2 cells. Each dot represents a gene. More gene-linked enhancers (<25 kb) show gains than show losses in accessibility.

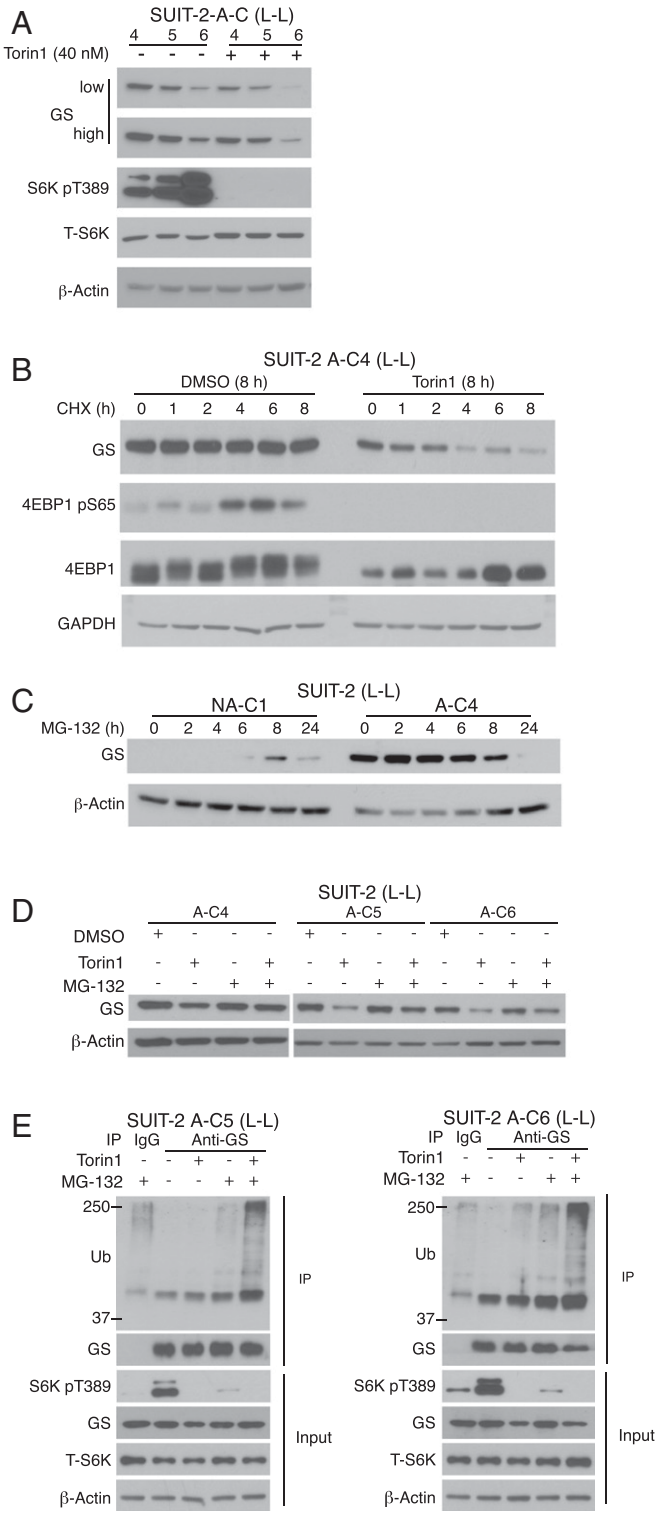

Fig. 5. mTORC1 stabilizes GS protein levels under glutamine deprivation. (*A*) Immunoblots of GS (low and high exposures), pT389-S6K, and total S6K in SUIT-2 adapted clones (C4 to C6) that were treated with vehicle control dimethyl sulfoxide (DMSO) or Torin 1 (40 nM) in L-L medium for 24 h. (*B*) Immunoblots of GS, pS65-4EBP1, and total 4EBP1 in SUIT-2 adapted clonal cells (A-C4) that were pretreated under L-L medium with control DMSO (all six lanes on the *Left*) or Torin 1 (200 nM, all six lanes on the *Right*) for a total of 8 h. Cycloheximide (CHX, 20 μg ml^{-1}) was either not added (0 h) or added as a cotreatment to the cells, for the indicated times (1, 2, 4, 6, or 8 h). (*C*) GS protein levels in nonadapted (C1) and adapted (C4) SUIT-2 clones treated in L-L medium with MG-132 (10 μM) for the indicated times. (*D*) GS protein levels in SUIT-2 adapted clones treated in L-L medium with either Torin 1 (200 nM) or MG-132 (10 μM) alone, or in combination for 12 h (C4) or 8 h (C5, C6). (*E*) Coimmunoprecipitation (IP) blots showing the ubiquitination status of GS in SUIT-2 adapted clones treated in L-L medium, with either Torin 1 (200 nM) or MG-132 (10 μM) alone, or in combination for 8 h. Input refers to immunoblots of total GS, pT389-S6K, and total S6K levels in whole cell lysates. In *A*–*E*, β-actin or GAPDH was used as loading control.

circulating glutamine, as sources of TCA cycle carbon (14, 35–37). This observation is supported by in vivo resistance of tumors to inhibitors of glutaminolysis (38). Differences in nutrient levels between cell culture media and human serum, in addition to the in vivo tumor environment, might partially explain this discrepancy (12, 39). However, although glutamate is a major source of TCA cycle carbon and nitrogen for transamination reactions and glutathione synthesis, glutamine per se is required for protein synthesis and is an indispensable source of amide nitrogen for nucleotide and hexosamine synthesis (34). Therefore, whereas proliferating tumor cells may resort to alternative sources of glutamate, such as transamination reactions instead of glutaminolysis, they can only survive in glutamine-deprived conditions if they can synthesize glutamine de novo.

Moreover, although glutamine may not seem to be depleted in extracts of whole tumors or tumor interstitial fluid (16), tumor cores hold lower levels than the periphery (19, 20). Thus, the precise location of a cancer cell within the hypoxic, stroma-dense tumor may dictate its dependence on glutamine at various times. Distinct clusters of tumor cells likely exist within PDA tumors with differential nutrient access depending on the proximity to blood vessels and density of the surrounding stroma. The deprivation of PDA tumor cells of nutrients may also change over time, as tumor growth reshapes 3D cellular organization and the proximity of cancer cells to stroma and endothelial cells. It is therefore not surprising that, unlike Bott et al. (34), we found no significant association between average GS levels and tumor grade or patient survival (*SI Appendix*, Fig. S13). We find instead that rare clonal cells are able to survive and adapt to low levels of the tumor-preferred nutrients glucose and glutamine; these cells induce glutamine synthesis, which is required for their growth in vitro and in vivo.

Despite chronic nutrient deprivation in the adapted cells, we find that activated mTORC1 induces GS. Although GS is known to be regulated posttranslationally (30, 31), the signaling basis for this regulation was unknown. We show that mTORC1 plays a key posttranslational role in stabilizing GS by preventing its ubiquitination and proteasomal degradation. mTORC1 inhibition was previously shown to enhance proteasomal degradation of long-lived proteins (40), but GS was not identified as a specific target, perhaps because the experiments were performed under glutamine-replete conditions. What induces mTORC1 activity in the absence of glucose and glutamine in adapted PDA cells is a question worthy of future investigation. One plausible explanation is that epigenetic alterations that occur upon adaptation to nutrient deprivation (Fig. 4 and *SI Appendix*, Fig. S10) may influence genes that directly or indirectly activate mTORC1 (*SI Appendix*, Fig. S4*G*).

We propose that PDA cells that survive and adapt to nutrient deprivation acquire an epigenetic state that endows them with the flexibility to switch between metabolic states that are optimal for growth under nutrient-replete or nutrient-deprived conditions. A key contributing factor to the adaptation to nutrient-depleted conditions is activation of mTORC1, which in turn stabilizes GS, thus enabling essential glutamine synthesis for pancreatic cancer growth (Fig. 6*F*). Consequently, targeting of GS, the expression of which is induced in nutrient-deprived cell clusters within PDA tumors, holds therapeutic benefit to pancreatic cancer patients.

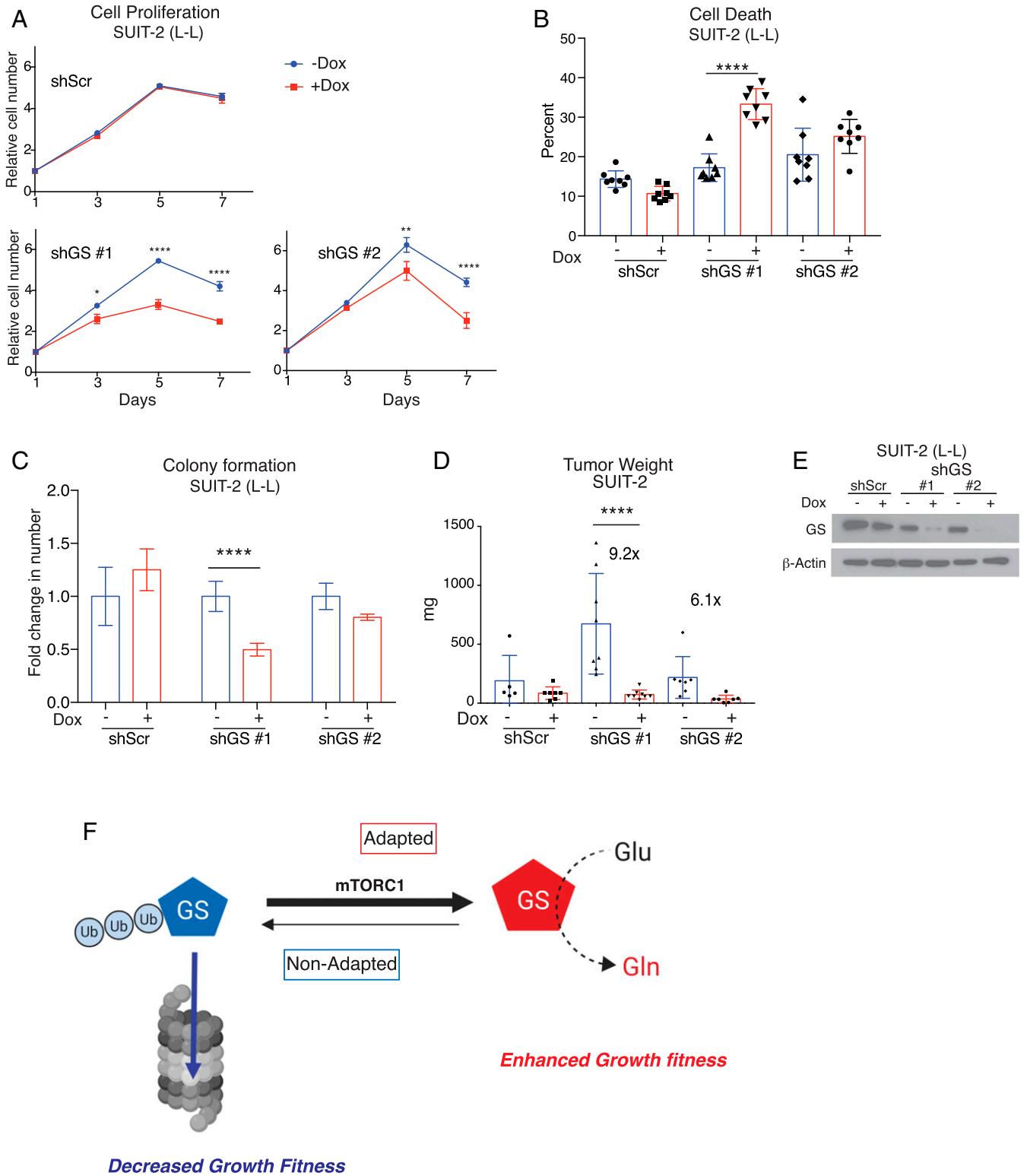

Fig. 6. GS is required for the adaptation-induced growth fitness of PDA cells under nutrient deprivation. (*A*) Proliferation curves of adapted SUIT-2 clonal cells transfected with Dox-inducible shScrambled control or shGS hairpins 1 and 2, grown in L-L medium for 7 d in the absence or presence of 1 μg ml^{-1} Dox ($n = 8$). (*B*) Percent cell death in cells described in *A* ($n = 8$) that were grown in L-L medium for 7 d. (*C*) Colony formation assay for cells in *A* that were grown for 10 d, under L-L conditions ($n = 6$). (*D*) Weights of orthotopic xenograft PDA tumors derived from SUIT-2 adapted cells (C4) stably expressing Dox-inducible hairpins described in *A* that were injected (750×10^3 cells) into the pancreas of 4- to 6-wk-old $Rag1^{-/-}$ mice. Dox was supplemented in the drinking water (2 mg ml^{-1}) 5 d postinjection of cells, and tumors were harvested 33 d later ($n = 5$ shScr −Dox; $n = 7$ shScr +Dox; $n = 8$ shGS#1; $n = 7$ shGS#2). Data represent the mean ± SEM in *A* and mean ± SD in *B*–*D*. $^*P < 0.05$; $^{**}P < 0.01$; $^{****}P < 0.0001$, two-way ANOVA followed by a Tukey test. (*E*) Immunoblots of GS in cells used for xenografts in *D* showing decreased protein levels, 48 h following treatment with Dox (1 μg ml^{-1}) for inducible knockdown. β-Actin was used as loading control. (*F*) Model illustrating a role for GS stabilization in PDA cell adaptation to nutrient deprivation, which leads to enhanced growth fitness. The sketch was created using Biorender.com.

Materials and Methods

All reagents, cell culture, transcriptional, epigenetic, metabolic, and animal studies as well statistical analysis are described in detail *SI Appendix, SI Materials and Methods*. Mouse studies were approved by the institutional animal care and use committee at Boston Children's Hospital.

Data Availability. The RNA-Seq, ATAC-Seq, and DNA-Seq (WES) data have been deposited in National Center for Biotechnology Information (NCBI)'s Gene Expression Omnibus and are accessible through GEO Series accession no. GSE144833.

ACKNOWLEDGMENTS. We thank members of the N.Y.K. laboratory and the Division of Endocrinology, Boston Children's Hospital, for helpful comments and discussions. This work was supported by American Cancer Society Research Scholar Grant RSG-17-070-01-TBG (to N.Y.K.) and by funds from Boston Children's Hospital. N.Y.K. is also supported by NIH/National Cancer Institute Grant R01 CA211944. P.-Y.T. was partly funded by a Top University Strategic Alliance fellowship from Taiwan. Work by M.M. and S.N. was supported by Harvard Catalyst, the Harvard Clinical and Translational Science Center (NIH Award UL1 RR 025758), and computations were run on the Orchestra cluster supported by the Harvard Medical School Research Computing Group.

1. R. L. Siegel, K. D. Miller, A. Jemal, Cancer statistics, 2020. *CA Cancer J. Clin.* **70**, 7–30 (2020).
2. L. Rahib *et al.*, Projecting cancer incidence and deaths to 2030: The unexpected burden of thyroid, liver, and pancreas cancers in the United States. *Cancer Res.* **74**, 2913–2921 (2014).
3. R. M. Perera, N. Bardeesy, Pancreatic cancer metabolism: Breaking it down to build it back up. *Cancer Discov.* **5**, 1247–1261 (2015).
4. H. Ying *et al.*, Genetics and biology of pancreatic ductal adenocarcinoma. *Genes Dev.* **30**, 355–385 (2016).
5. S. Yang *et al.*, Pancreatic cancers require autophagy for tumor growth. *Genes Dev.* **25**, 717–729 (2011).
6. C. Commisso *et al.*, Macropinocytosis of protein is an amino acid supply route in Ras-transformed cells. *Nature* **497**, 633–637 (2013).
7. J. J. Kamphorst *et al.*, Human pancreatic cancer tumors are nutrient poor and tumor cells actively scavenge extracellular protein. *Cancer Res.* **75**, 544–553 (2015).
8. O. Olivares *et al.*, Collagen-derived proline promotes pancreatic ductal adenocarcinoma cell survival under nutrient limited conditions. *Nat. Commun.* **8**, 16031 (2017).
9. H. Ying *et al.*, Oncogenic Kras maintains pancreatic tumors through regulation of anabolic glucose metabolism. *Cell* **149**, 656–670 (2012).
10. J. Son *et al.*, Glutamine supports pancreatic cancer growth through a KRAS-regulated metabolic pathway. *Nature* **496**, 101–105 (2013).
11. A. Muir, M. G. Vander Heiden, The nutrient environment affects therapy. *Science* **360**, 962–963 (2018).
12. S. M. Davidson *et al.*, Environment impacts the metabolic dependencies of ras-driven non-small cell lung cancer. *Cell Metab.* **23**, 517–528 (2016).
13. C. T. Hensley *et al.*, Metabolic heterogeneity in human lung tumors. *Cell* **164**, 681–694 (2016).
14. E. A. Maher *et al.*, Metabolism of [U-13 C]glucose in human brain tumors in vivo. *NMR Biomed.* **25**, 1234–1244 (2012).
15. I. Marin-Valencia *et al.*, Analysis of tumor metabolism reveals mitochondrial glucose oxidation in genetically diverse human glioblastomas in the mouse brain in vivo. *Cell Metab.* **15**, 827–837 (2012).
16. M. R. Sullivan *et al.*, Quantification of microenvironmental metabolites in murine cancers reveals determinants of tumor nutrient availability. *eLife* **8**, e44235 (2019).
17. J. R. Cantor *et al.*, Physiologic medium rewires cellular metabolism and reveals uric acid as an endogenous inhibitor of UMP synthase. *Cell* **169**, 258–272.e17 (2017).
18. J. Vande Voorde *et al.*, Improving the metabolic fidelity of cancer models with a physiological cell culture medium. *Sci. Adv.* **5**, eaau7314 (2019).
19. M. Pan *et al.*, Regional glutamine deficiency in tumours promotes dedifferentiation through inhibition of histone demethylation. *Nat. Cell Biol.* **18**, 1090–1101 (2016).
20. S. W. Lee *et al.*, EGFR-pak signaling selectively regulates glutamine deprivation-induced macropinocytosis. *Dev. Cell* **50**, 381–392.e5 (2019).
21. N. Psychogios *et al.*, The human serum metabolome. *PLoS One* **6**, e16957 (2011).
22. B. J. Altman, Z. E. Stine, C. V. Dang, From Krebs to clinic: Glutamine metabolism to cancer therapy. *Nat. Rev. Cancer* **16**, 749 (2016).
23. T. Gebregiworgis *et al.*, Glucose limitation alters glutamine metabolism in MUC1-overexpressing pancreatic cancer cells. *J. Proteome Res.* **16**, 3536–3546 (2017).
24. H. W. S. Tan, A. Y. L. Sim, Y. C. Long, Glutamine metabolism regulates autophagy-dependent mTORC1 reactivation during amino acid starvation. *Nat. Commun.* **8**, 338 (2017).
25. L. Yan, P. Raj, W. Yao, H. Ying, Glucose metabolism in pancreatic cancer. *Cancers (Basel)* **11**, 1460 (2019).
26. I. Ben-Sahra, J. J. Howell, J. M. Asara, B. D. Manning, Stimulation of de novo pyrimidine synthesis by growth signaling through mTOR and S6K1. *Science* **339**, 1323–1328 (2013).
27. L. S. Harrington *et al.*, The TSC1-2 tumor suppressor controls insulin-PI3K signaling via regulation of IRS proteins. *J. Cell Biol.* **166**, 213–223 (2004).
28. P. P. Hsu *et al.*, The mTOR-regulated phosphoproteome reveals a mechanism of mTORC1-mediated inhibition of growth factor signaling. *Science* **332**, 1317–1322 (2011).
29. O. J. Shah, Z. Wang, T. Hunter, Inappropriate activation of the TSC/Rheb/mTOR/S6K cassette induces IRS1/2 depletion, insulin resistance, and cell survival deficiencies. *Curr. Biol.* **14**, 1650–1656 (2004).
30. T. V. Nguyen *et al.*, Glutamine triggers acetylation-dependent degradation of glutamine synthetase via the thalidomide receptor cereblon. *Mol. Cell* **61**, 809–820 (2016).
31. T. V. Nguyen *et al.*, p97/VCP promotes degradation of CRBN substrate glutamine synthetase and neosubstrates. *Proc. Natl. Acad. Sci. U.S.A.* **114**, 3565–3571 (2017).
32. S. L. Klemm, Z. Shipony, W. J. Greenleaf, Chromatin accessibility and the regulatory epigenome. *Nat. Rev. Genet.* **20**, 207–220 (2019).
33. P. J. Allen *et al.*, Multi-institutional validation Study of the American joint commission on cancer (8th edition) changes for T and N staging in patients With pancreatic adenocarcinoma. *Ann. Surg.* **265**, 185–191 (2017).
34. A. J. Bott *et al.*, Glutamine anabolism plays a critical role in pancreatic cancer by coupling carbon and nitrogen metabolism. *Cell Rep.* **29**, 1287–1298.e6 (2019).
35. M. O. Yuneva *et al.*, The metabolic profile of tumors depends on both the responsible genetic lesion and tissue type. *Cell Metab.* **15**, 157–170 (2012).
36. S. Tardito *et al.*, Glutamine synthetase activity fuels nucleotide biosynthesis and supports growth of glutamine-restricted glioblastoma. *Nat. Cell Biol.* **17**, 1556–1568 (2015).
37. S. H. Issaq, A. Mendoza, S. D. Fox, L. J. Helman, Glutamine synthetase is necessary for sarcoma adaptation to glutamine deprivation and tumor growth. *Oncogenesis* **8**, 20 (2019).
38. D. E. Biancur *et al.*, Compensatory metabolic networks in pancreatic cancers upon perturbation of glutamine metabolism. *Nat. Commun.* **8**, 15965 (2017).
39. A. Muir *et al.*, Environmental cystine drives glutamine anaplerosis and sensitizes cancer cells to glutaminase inhibition. *eLife* **6**, e27713 (2017).
40. J. Zhao, B. Zhai, S. P. Gygi, A. L. Goldberg, mTOR inhibition activates overall protein degradation by the ubiquitin proteasome system as well as by autophagy. *Proc. Natl. Acad. Sci. U.S.A.* **112**, 15790–15797 (2015).